INVESTIGATION ON THERMAL PERFORMANCE OF ZEOLITE PARTICLES AS POTENTIAL INSULATORS

Le Minh Tam*, Nguyen Van Quy
University of Technology and Education, Ho Chi Minh City

ARTICLE INFO

Received: 12/4/2024
Revised: 31/5/2024
Published: 31/5/2024

KEYWORDS

Zeolite
Kaolin
Heat conductivity
Heat insulator
Porous materials

ABSTRACT

This study presents the results of the thermal performance of two different zeolites in heat absorption and heat release investigated under multiple heating-cooling cycles. The specific focus is highlighting the influence of zeolitic structure in comparison to the raw kaolin as their precursor to evaluate the role of porous materials. Kaolin is a naturally occurring mineral lacking a porous structure, which conducts heat through typical solid material mechanisms and quickly equilibrates with the temperature of the surroundings. In contrast, the porous nature of zeolite creates abundant air-filled cavities, which establish a thermal buffer zone leading to temperature discrepancies with the environment. At the equilibrium state at 70 ^{o}C, zeolite Y exhibits a temperature buffer of 3.5 °C, while zeolite 4A demonstrates a smaller difference of 2.2 °C. These findings are consistent with the research on porous volumes of the synthesized zeolite Y (3.59×10^{-2} cm^3 g^{-1}) and zeolite 4A (1.85×10^{-2} cm^3 g^{-1}). In the estimation section, heat conductivity coefficients and specific heat capacities of these materials were determined which resulted in good agreements with heat behavior of these zeolitic materials. Consequently, the applicability of these zeolites as external insulators can be expected if the thickness of the material layers is optimized according to the intended temperature range.

NGHIÊN CỨU HIỆU NĂNG NHIỆT CỦA CÁC HẠT ZEOLITE ỨNG DỤNG LÀM CHẤT CÁCH NHIỆT

Lê Minh Tâm*, NguyễnVăn Quý
Trường Đại học Sư phạm Kỹ thuật - Thành phố Hồ Chí Minh

THÔNG TIN BÀI BÁO

Ngày nhận bài: 12/4/2024
Ngày hoàn thiện: 31/5/2024
Ngày đăng: 31/5/2024

TỪ KHÓA

Zeolite
Cao lanh
Dẫn nhiệt
Cách nhiệt
Vật liệu xốp

TÓM TẮT

Nghiên cứu này trình bày kết quả về hiệu năng của hai loại zeolite trong việc hấp thụ và giải phóng nhiệt, được nghiên cứu dưới nhiều chu trình làm nóng và làm lạnh. Trọng tâm của nghiên cứu nhằm nhấn mạnh ảnh hưởng của sự khác biệt về cấu trúc zeolite so với kaolin. Kaolin là một khoáng vật tự nhiên dẫn nhiệt theo cơ chế của vật liệu rắn điển hình và nhanh chóng cân bằng với nhiệt độ của môi trường xung quanh. Ngược lại, tính chất xốp của zeolite hoạt động như các khoang chứa khí, tạo nên một vùng đệm nhiệt dẫn đến sự chênh lệch nhiệt độ với môi trường. Ở trạng thái cân bằng tại 70 °C, zeolite Y thể hiện một vùng đệm nhiệt là 3,5 °C, trong khi zeolite 4A cho thấy một sự khác biệt nhỏ hơn là 2,2 °C. Những kết quả này tương thích với nghiên cứu về tính chất xốp của zeolite, cụ thể là thể tích xốp của zeolite Y ($3,59 \times 10^{-2}$ cm^3 g^{-1}) và zeolite 4A ($1,85 \times 10^{-2}$ cm^3 g^{-1}). Ngoài ra, hệ số dẫn nhiệt và nhiệt dung riêng của các vật liệu này đã được xác định và cho kết quả phù hợp với hành vi nhiệt của chúng. Do đó, khả năng áp dụng của các zeolite này làm lớp cách nhiệt bên ngoài có thể đạt được khi bề dày của chúng được tối ưu hóa.

DOI: https://doi.org/10.34238/tnu-jst.10137

* Corresponding author. *Email: tamlm@hcmute.edu.vn*

1. Introduction

Global warming is currently the major problem of sustainable development worldwide that requires new generations of more effective heat insulators [1] – [3]. Furthermore, the circular economy demands urgent attention to the efficient use of energy types and the exploitation of renewable energy sources to replace non-renewable ones [4] – [6]. Energy saving based on advanced materials is a sustainable solution [7], [8]. In tropical countries with year-round hot climates, the use of insulation materials to ensure a temperate climate in households is widely addressed [9], [10]. In U.S., more than 48% of building energy consumption is to support cooling and heating systems [11]. In European and North American countries, the energy consumed for heating and subsequent loss to the environment is very high [12]. This is also a potential market for insulation materials. In recent decades, the use of PU foam and its derivatives has provided good thermal and acoustic insulation efficiency [13] – [15]. However, these materials are highly flammable, posing a potential risk of fire and explosion [15], [16]. Additionally, there are environmental pollution issues associated with the production of these materials [17]. Therefore, alternatives as inorganic insulation materials are a good choice in terms of both thermal performance and fire prevention. Among inorganic matters, zeolite is one of the prospective materials.

Zeolites are crystalline aluminosilicates with unique framework, which are extensively utilized owing to their high porosity and super light-weight. Numerous investigations focus on both natural and synthetic zeolites [18], [19]. The three-dimensional architecture of zeolites comprises interconnected tetrahedral silicate and aluminum units linked by oxygen atoms. Figure 1 presents structure of two typical zeolite types, e.g. sodalite and faujasite [20], [21]. Due to their porous nature, zeolites find widespread application in various fields such as agriculture, ecology, rubber, medicine and construction industries, household products, etc. primarily attributed to their exceptional adsorption properties [22], [23]. Additionally, due to its framework structure as porous materials, zeolite holds great potential as a thermal insulation material. This once again enables zeolite to be used alongside insulation layers in freezers, insulation panels for construction projects, external walls, and also as various coatings for thermal insulation. Furthermore, the heat absorption and heat release capabilities of zeolite are highly worthy of research. The hybrid nature of solid material and gas bubbles captured within its porous structure leads to the special thermal properties of zeolite, which is an area not fully understood and needs further investigation.

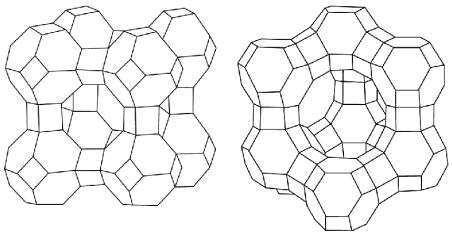

Figure 1. *Porous structure of zeolites in cases of sodalite (left) and faujasite (right)* [21], [22]

In this study, we use kaolin as a precursor to synthesize two types of zeolite with different structural properties. These three materials will be investigated for their heat performance in heat absorption and heat release. Uniform temperature cycling loops will be applied to all three samples to compare their ability to delay temperature rise as well as the rate of heat dissipation in response to changes in environmental temperature. Thus, we aim to establish the relationship between thermal properties and material structure when they transform from amorphous to various crystalline structures. In parallel with experimentation, the development of a mathematical model will also contribute to creating robust research tools computing heat conductivity coefficients and specific heat capacity. This model complements experiments, enabling predictions for areas where experiments are challenging.

2. Materials and Methods

2.1. Mathematical equations

Herein, we describe heat transfer behavior in a hollow cylindrical object that has dimensions of (r_1, r_2, L are outer, inner radius and length with values of 10 × 2.5 × 40 mm) as plotted in Figure 2. Since the length of this object predominates the radius, the heat transfer according to radial direction is interested.

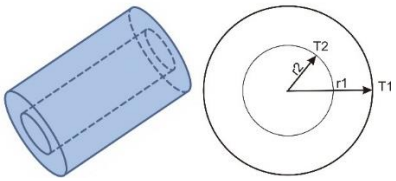

Figure 2. *Heat conduction in cylindrical object with dimensions $r_1 \times r_2 \times L$. T_1 and T_2 stand for temperatures at r_1 and r_2 positions*

At steady state, equation (1) is applied for element r + Δr. Take the limit as $\Delta r \to 0$, this leads to the simple differential equation (2). From Fourier's law, the heat flux is calculated in the radial direction as Equation (3), in which the term A is the area of the cylindrical surface. Transforming Equation (4) and integrating Equation (5) result in Equation (6). Using boundary conditions as in Equation (7), integration constants C_1 and C_2 are obtained as Equations (8) and (9). We are ready to evaluate the heat flow rate Q as Equation (10). Finally, rearrangement gives us Equation (11) for the heat flow rate transfers into the cylindrical shell.

$$\frac{Q(r+\Delta r)-Q(r)}{\Delta r}=0 \quad (1)$$

$$\frac{dQ}{dr}=0 \quad (2)$$

$$-Ak\frac{dT}{dr}=-2\pi rLk\frac{dT}{dr}=const. \quad (3)$$

$$r\frac{dT}{dr}=C_1 \quad (4)$$

$$dT=C_1\frac{dr}{r} \quad (5)$$

$$T=C_1\ln(r)+C_2 \quad (6)$$

$$T(r_1)=T_1;T(r_2)=T_2 \quad (7)$$

$$C_1=\frac{(T_1-T_2)}{ln\frac{r_1}{r_2}} \quad (8)$$

$$C_2=T_1-\frac{(T_1-T_2)}{ln\frac{r_1}{r_2}}lnr_1 \quad (9)$$

$$Q=q_rA=\left(-k\frac{dT}{dr}\right)2\pi rL=(-kC_1)2\pi L \quad (10)$$

$$Q=2\pi Lk\frac{T_1-T_2}{ln\frac{r_2}{r_1}} \quad (11)$$

$$Q=mC_p(T-T') \quad (12)$$

2.2. Estimation procedure

To calculate heat flow rate into the cylindrical shell, there are two parameters needed to be estimated, including k (heat conductivity) in Equation (11) and C_p (specific heat capacity) in Equation (12). The parameter estimation procedure is performed using a Matlab function ***fminsearch***, which allow minimizing the objective function OF (13) (error < 10^{-9}) for n points, k is the index. This function is defined as the difference between Q values in Equations (11) and (12). Herein, T is assumed as average of T_1 and T_2 while T' stands for the initial environment temperature.

$$OF=\sum_{k=1}^{n}\left(2\pi Lk\frac{T_1-T_2}{ln\frac{r_2}{r_1}}-mC_p(T-T')\right)^2 \quad (13)$$

2.3. Zeolite synthesis via hydrothermal reactions

Similar routes to the literature [24] were applied to synthesize zeolite via the hydrothermal method at high temperature and pressure. Herein, the procedure was briefly summarized as follows. From the original source of kaolin, we analyzed the components present in kaolin. Kaolin was heated at 900 °C for 2 hours to break down the structure of kaolin, removed chemically bound water, and transformed kaolin into metakaolin. For each type of zeolite, there were corresponding gel formulations (xNa_2O: yAl_2O_3: $zSiO_2$: tH_2O). Then, the blending ratios for each type of zeolite were calculated. Water and NaOH were weighed. A portion of water was added to NaOH, and stirred until all NaOH was dissolved. Metakaolin and NaOH solution were stirred for 5 minutes without heating. The next steps involve weighing Na_2SiO_3 (if additional $SiO_2$was needed) or $AlCl_3$ (if additional Al_2O_3 was needed), adding the remaining water, and stirring to dissolve. Then, Na_2SiO_3 or $AlCl_3$ solution was added to the container containing NaOH solution, and metakaolin was being stirred. Continue stirring this mixture to form a homogeneous gel. Aging the gel by continuous stirring at room temperature for a period of 24 hours. Thermal crystallization in an autoclave was conducted for 9h. After crystallization, it was allowed to cool down to room temperature. To remove alkali, vacuum filtered and washed steps for the obtained crystals with distilled water until reaching a neutral pH were carried. Dry overnight at 60°C, zeolites were yielded.

2.4. Experimental set up for heat response investigation

First, three thermocouples namely (1), (2), and (3) were set up as shown in Figure 3. The first one measured the surrounding temperature (T_1) directly outside of the measured sample. The second one was positioned at the center of the sample to measure T_2. Finally, the sensor (3) was connected to the PID unit to automatically control the temperature inside the measurement chamber. The sample was fully filled with powder of kaolin or zeolites. The chamber was programmed with a heating rate of 5 $^oC\ min^{-1}$ and naturally cooling with ambient conditions. A wolfram lamb was used as a heat source as shown in Figure 3. Each heating or cooling period was kept for 30 minutes.

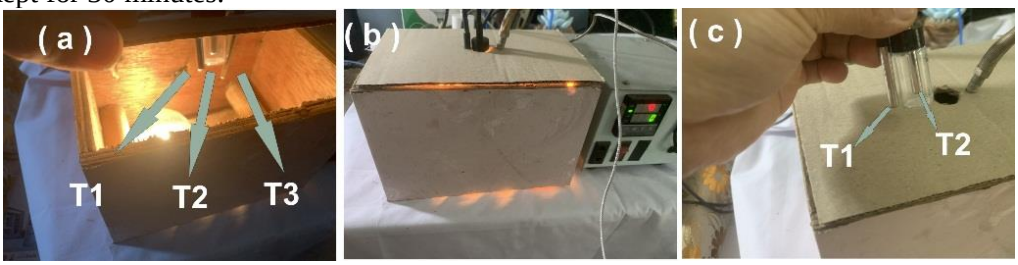

Figure 3. *Experimental setup, T_1 and T_2 stand for outer and inner sample temperatures while T_3 is the sensor connected to the PID control. The powder was filled into the vessel before immersing sensor T_2 into the sample*

3. Results and Discussion

3.1. Effects of temperature and initial composition in zeolite synthesis

Starting with the same precursor kaolin (Figure 4a, b), the synthesized products can be varied significantly depending on reaction conditions. Among these conditions, temperature and initial ratio of reactants are two crucial factors. With the results summarized in Table 1, the zeolite 4A was obtained after crystallization at 90 ^oC which is actually similar to the synthesis conditions mentioned in the literature [24]. In Figure 4c-d, these cubic crystals are typical morphology of zeolite 4A of which crystal structure belongs to group of sodalite family as presented in Figure 1. The particle size of these crystals is rather homogeneous and range from 2 to 5 μm. Their porous

properties were listed in Table 2. A ratio of Al : Si at ~1.2 was found which is belongs to the typical range of zeolite 4A [20].

Table 1. *Synthesized zeolite 4A and Y*

Products	Unit	Zeolite 4A	Zeolite Y
Temperature	^{o}C	90	100
Reaction time	h	9	9
Al content	%	14.39	15.42
Si content	%	11.7	9.26
Ratio of Al/Si	-	1.19	1.61
Average particle size	µm	3.75	1.14

Under the same scenarios but temperature being raised to 100 ^{o}C, the product crystalized as Y zeolite which shows a completely different morphology as seen in Figure 4e-f. They are much smaller particles than the case of zeolite 4A with an average particle size of about 1.14 µm. Finally, the ratio of Al : Si at a value of 1.6 is typical for faujasite zeolitic materials (see Figure 1) [21]. Thus, we have successfully synthesized two different zeolites, i.e. types of 4A and Y which will be further used to examine their heat behavior in the next sections.

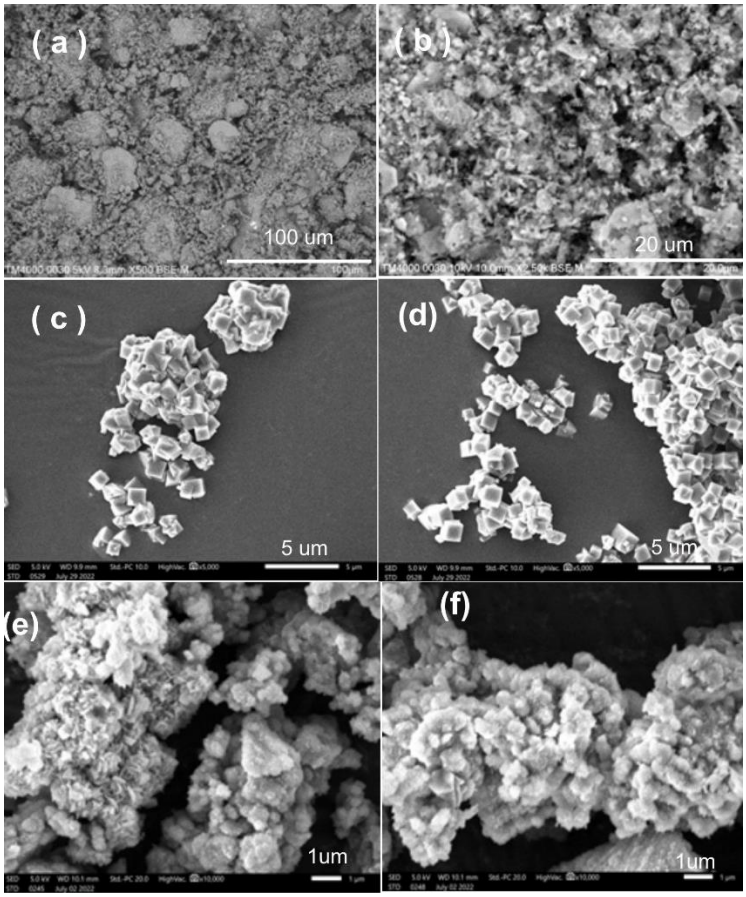

Figure 4. *SEM images of (a) and (b) – precursor kaolin as amorphous material; (c) and (d) for zeolite 4A; (e) and (f) – for zeolite Y. (the scale diameters were resembled for readability)*

3.2. Texture properties via BET measurement

These two obtained zeolites were subjected to porosity analysis of which the results were summarized in Table 2. Obviously, these two zeolites are porous materials but 4A exhibits

relatively low porosity compared to the zeolite Y. Indeed, the porous properties are distinguishable enough to subject them in heat differential behavior investigation. The porous volume of 4A was found at 1.86×10^{-2} $cm^3 g^{-1}$ which is lower than that of zeolite Y at 3.59×10^{-2} $cm^3 g^{-1}$. Besides, the surface area of Y is also higher than the case of 4A with values at 65.16 $m^2 g^{-1}$ and 5.60 $m^2 g^{-1}$, respectively. These could be the major factors deciding their heat performance difference as thermal insulation materials. In short, zeolite Y shows more advantages than the 4A type in potential heat application since it creates more air-filled cavities.

Table 2. *Porosity of the synthesized zeolites*

Properties	Unit	4A	Y	kaolin
BET Surface Area	$m^2 g^{-1}$	5.60	65.16	0.74
Pore Volume	$cm^3 g^{-1}$	1.86×10^{-3}	3.59×10^{-3}	3.82×10^{-4}

3.3. Heat responses of kaolin and zeolite

3.3.1. Study on Kaolin

First, the material response to heating and cooling cycles is introduced in Figure 5a. The first cycle (green-marked rectangular) was selected to describe the involved events. Under a heating rate of 5 $^oC\ min^{-1}$, the outer temperature of the sample T_1 (red-curve) increases rapidly from 30 to 70 ^oC for 700 seconds. Simultaneously, the inner temperature of the sample T_2 (black-curve) behaves analogues with a delayed temperature recorded as $\Delta T = T_2 - T_1$ which was also plotted in Figure 5b. In this case, the maximal discrepancy reached a value of 11.6 ^oC after 90 seconds. Consequently, both T_1 and T_2 curves were plateaued since they reached equilibrium state which gives the thermal buffer capacity of the studied material. When the heat source was cut off, T_1 decreased faster than T_2 since heat flux was gradually reversely released from inside to the surroundings. Then, these two curves of kaolin were identical when time was prolonged as seen in the 5th cycle. Observing all five cycles, it is evident that these cycles had almost the same behavior which proved excellent repeatability of the system with an error less than 12% (comparing the individual to the average numbers). Thus, the experimental system exhibits high reliability and could be suggested for further investigation.

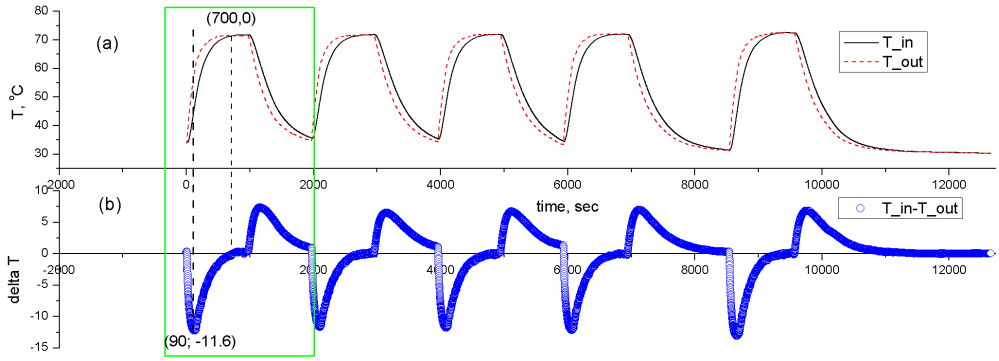

Figure 5. *Cyclic heating and cooling response of kaolin*

A particularly notable finding across all heat cycles is the presence of a delay between the current temperature of the environment (T_1) and the temperature at the r_2 position of the measurement cell (T_2) due to thermal resistance and the heat transfer process from the walls to the r_2 position of the equipment. For instance, the maximum difference can reach 11.6 °C after 90 seconds, as depicted in Figure 5b. However, over a sufficiently long period, this difference gradually diminishes and approaches 0.2 °C. Thus, the temperature of the environment and the temperature at the core of the measurement cell become equal. This indicates the poor thermal

insulation effects of kaolin that is consistent with non-porosity property of this material listed in Table 2. Thus, if the duration is extended to equilibrium, kaolin will lose its insulation ability.

Table 3. *Maximal discrepancy and temperature buffer of kaolin.*

Cycle	1st	2nd	3rd	4th	5th
$\lfloor T_2 - T_1 \rfloor$max	11.62	11.44	11.37	12.13	12.75
$\lfloor \Delta T_{equilibrium} \rfloor$	0.19	0.20	0.22	0.21	0.18
Error, %	4.04	5.05	11.11	6.06	9.09

3.3.2. Study on Zeolite 4A

Figure 6 shows that the zeolite 4A exhibits a similar thermal response as kaolin does. However, its thermal conductive rate is slower than in the previous case, which results in temperature discrepancies. This can be explained based on the porous structure of zeolite 4A. According to BET analysis in Table 2, zeolite 4Ais a porous material. Indeed, its surface area is 5.6 $m^2 g^{-1}$, and its porous volume is 1.86×10^{-2} $m^3 g^{-1}$. Consequently, the insulation property of zeolite 4A will be enhanced by the air-buffering effects compared to kaolin.

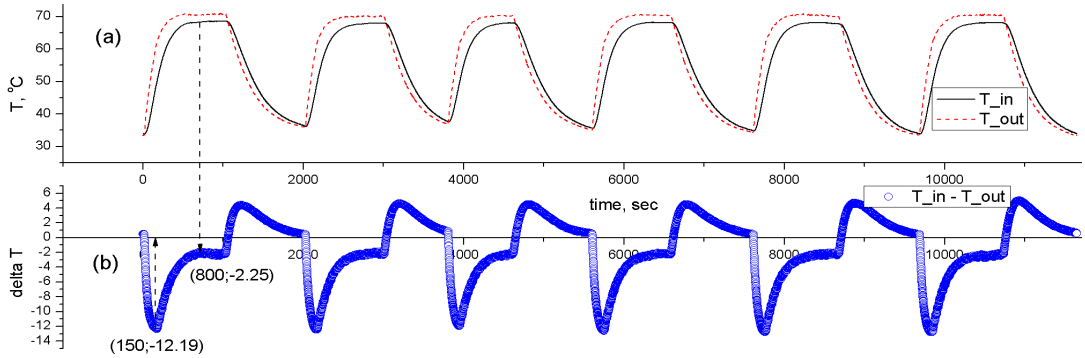

Figure 6. *Heat response of zeolite 4A*

Table 4 details the major differences of the 6 heating-cooling loops. For instance, the 1st run, after about 150 seconds, the maximal temperature delay to the surrounding of zeolite 4A reached 12.2 °C compared to kaolin is 11.6 °C. The system reached equilibrium after 800 sec and remained a discrepancy of about 2.3 °C while this difference in the case of kaolin is 0.2 °C. Thus, zeolite 4A possesses better insulation property than that of kaolin. Thus, it can be used for construction as an external insulator.

Table 4. *Heat difference and heat buffer of zeolite 4A*

Cycle	1st	2nd	3rd	4th	5th	6th
$\lfloor T_2 - T_1 \rfloor$max	12.19	12.25	11.81	12.57	12.5	12.63
$\lfloor \Delta T_{equilibrium} \rfloor$	2.25	2.37	2.25	1.82	2.00	2.18
Error, %	4.89	10.48	4.89	15.15	6.75	1.63

3.3.3. Study on Zeolite Y

In the two previous cases we known that the system possesses outstanding repeatability. Thus, just few cycles were needed to perform in this part. Zeolite Y demonstrates exceptional thermal insulating properties. As seen in the first loop in Figure 7, the maximum temperature delay during the heating cycle reached 15 °C after 170 seconds. Following this, the system gradually attained equilibrium after more than 1000 seconds. At the end of each cycle, the temperature difference induced comparing to the surroundings is 3.3 °C (the average for 3 cycles was 3.5 °C).

This outcome holds great promise for the utilization of this zeolite type in applications such as thermal insulation.

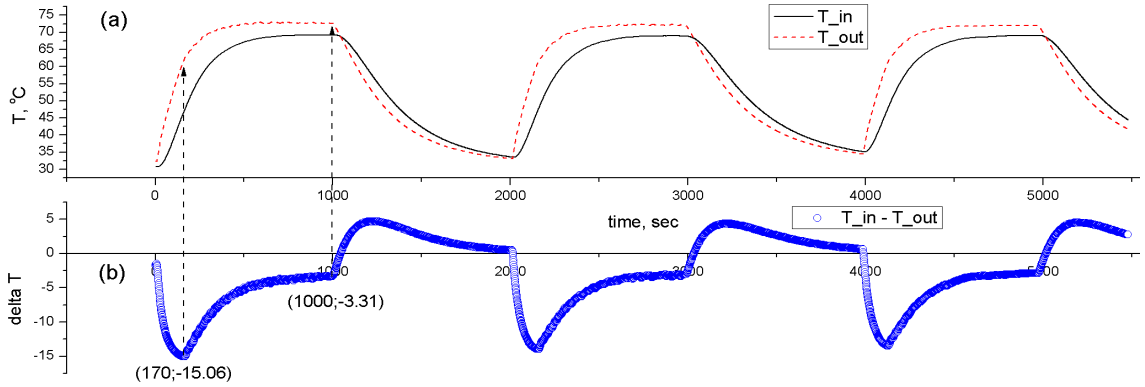

Figure 7. *Heat response for zeolite Y*

Results for 3 cycles were summarized in Table 5. Obviously, the good insulation phenomenon of zeolite Y can be accounted for the porous framework structure characteristic of this zeolite type. Unlike kaolin, which lacks porosity, BET analysis demonstrates the remarkable porous nature of zeolite compared to kaolin and zeolite 4A. The surface area was measured at 65.16 m^2 g^{-1} while the pore volume was found at a value of 3.59×10^{-2} cm^3 g^{-1}. Consequently, the air-filled cavities within zeolite serve as a thermal buffer and create an ideal thermal insulation material.

Table 5. *Difference between inner and outer temperatures for zeolite Y*

Cycle	1st	2nd	3rd
$[T_2 - T_1]$max	15.06	13.94	13.44
$\lfloor \Delta T_{equilibrium} \rfloor$	3.31	3.56	3.68
Error, %	5.87	1.23	4.64

Interestingly, according to cooling branches of the three materials, it shows that the heat release rate is also affected by material porosity which is listed in Table 2. Figure 8 illustrates a comparative analysis of the heat release rates among the three materials.

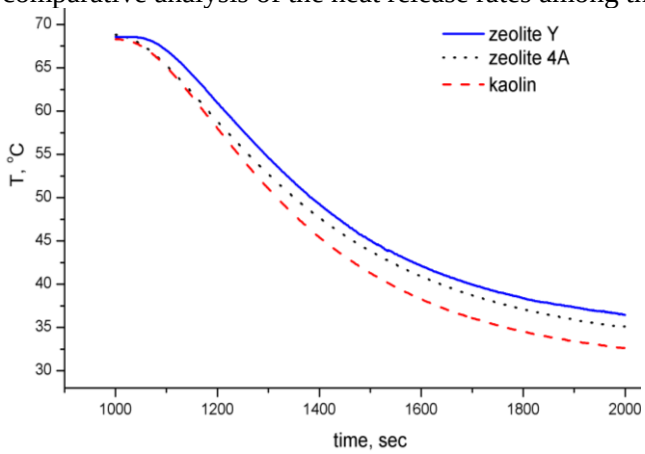

Figure 8. *Heat release of kaolin (red curve), zeolite 4A (blue curve), and zeolite Y (black curve)*

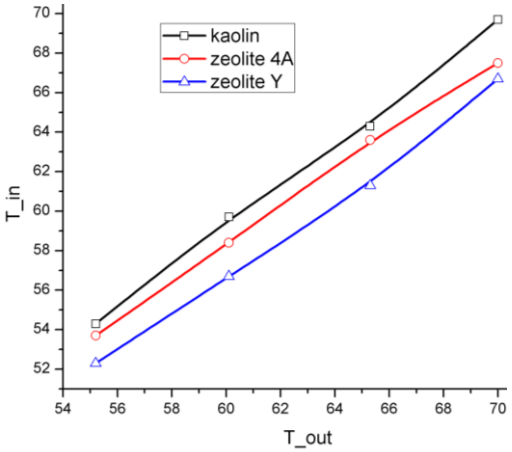

Figure 9. *Response of inner temperature according outer temperature variation*

Notably, kaolin demonstrates not only the swiftest heating cycle but also exhibits the highest rate of heat release (see red curve in Figure 8). Following closely is zeolite 4A (black curve), while zeolite Y (blue curve) possesses the slowest heat release rate. These phenomena are in a

good agreement with the porosity of these materials listed in Table 2 in which zeolite Y has higher pore volume and surface area than those of the zeolite 4A. Since kaolin is a nonporous material then its energy is quickly transferred in both heating and cooling cycles.

3.4. Heat conductivity coefficient and specific heat capacity estimation

Similar procedures to the previous cases but outer temperatures (T_1) were consecutively changed from 55 ^oC to 70 ^oC to measure the response of inner temperature (T_2). For three types of materials, the resulting T_2 were presented as functions of T_1 as seen in Figure 9.

Applying estimation technique as described in Equation (13), two parameters were obtained including heat conductivity (k) and specific heat capacity (C_p) which were summarized in Table 6. First, kaolin possesses relatively large heat conductivity coefficient k = 0.808 W m^{-1} $^oC^{-1}$ which much higher than those of zeolites 4A and Y at values of 0.227 W m^{-1} $^oC^{-1}$ and 0.121 W m^{-1} $^oC^{-1}$, respectively. It means that among these materials, kaolin response fastest to the temperature change of the environment. Along with its nonporous property, it is reasonable that kaolin quickly reaches the environment temperature as discussed in Figure 5. Thus, kaolin does not create thermal buffer effects. Furthermore, specific heat capacity of kaolin is also the smallest value (Cp = 1.007 kJ kg^{-1} $^oC^{-1}$) among these materials.

Heat conductivity coefficients of zeolites were found in a suitable range, which agreed with some reports in the literature [25], [26]. Herein, the role of porosity again shows a relationship with the heat response of the zeolitic materials. For instance, on the one hand, the pore volume of zeolite Y (3.59×10^{-2} cm^3 g^{-1}) is higher than that of zeolite 4A ($\times 10^{-2}$ cm^3 g^{-1}). On the other hand, the heat conductivity coefficient of zeolite Y is lower than that of the zeolite 4A with values of 0.121 W m^{-1} $^oC^{-1}$ and 0.227 W m^{-1} $^oC^{-1}$, respectively. Thus, the abundant air-filled cavities in zeolite Y enhance thermal resistor property, which helps zeolite Y act as a good thermal insulator. Additionally, the specific heat capacity of zeolite 4A was found at 1.240 kJ kg^{-1} $^oC^{-1}$ which is lower than that of zeolite Y at a value of 1.344 kJ kg^{-1} $^oC^{-1}$.

Table 5. *Estimation results of k and Cp*

Materials	**Heat conductivity**	**Confidence interval**	**Specific heat capacity**	**Confidence interval**
Unit	W m^{-1} $^oC^{-1}$		kJ kg^{-1} $^oC^{-1}$	
Zeolite Y	0.121	± 0.003	1.344	± 0.004
Zeolite 4A	0.227	± 0.001	1.240	± 0.004
Kaolin	0.808	± 0.006	1.032	± 0.006

For comparison purpose, the major results were summarized in Table 6. Obviously, the heating rate of these materials follows the order of kaolin > zeolite 4A > zeolite Y while the cooling rate shares a similar order as the heating rates.

Table 6. *Comparing heat release rate of the three materials for the first cooling cycles*

Materials	**Unit**	**Kaolin**	**Zeolite 4A**	**Zeolite Y**
$\tau(\Delta T_{max})$	sec	90	150	170
$\lfloor T_2 - T_1 \rfloor$max	^oC	11.6	12.2	15.0
$\tau(equi.)$	sec	700	800	1000
$\lfloor \Delta T_{equilibrium} \rfloor$	^oC	0.2	2.3	3.2

4. Conclusion

The heat absorbing and releasing processes demonstrated good repeatability for all three material types. With minor errors, it can be inferred that the research system exhibits high reliability, and the thermal characteristics align consistently with these investigated inorganic materials. Kaolin exhibits a rapid heat transfer phenomenon, so it reaches surrounding

temperature upon equilibrium. The explanation is attributable to its non-porous nature, thereby rendering its thermal insulation efficient. Conversely, based on porous structures, zeolites have developed air-filled cavities that enhance their thermal insulation properties. Notably, zeolite Y demonstrates a difference between the outer and inner chamber temperatures at a value of ~3.5°C, while zeolite 4A exhibits a smaller difference of ~2.3 °C. Assessment of parameters associated with material thermal properties has led to equivalent findings. The highest heat conductivity coefficient was observed in kaolin, with a value of 0.808 W m^{-1} $^oC^{-1}$, whereas zeolite 4A and zeolite Y exhibited lower values of 0.227 W m^{-1} $^oC^{-1}$ and 0.121 W m^{-1} $^oC^{-1}$, respectively. Regarding the potential utilization of these micro-porous materials as thermal insulators, the studied zeolites offer a good heat buffering capacity which supports their applicability to civil engineering projects. Optimization strategies such as adjusting material layer thickness can further enhance this buffering capability to meet the specific requirements of individual projects.

Acknowledgments

The author would like to thank HCMUTE for their support to carry out this study. We also would like to thank Ly Lam and Ho Thanh Quy for their help in experimental works.

REFERENCES

[1] N. W. Arnell and S. N. Gosling, "The impacts of climate change on river flood risk at the global scale," *Clim Chang*, vol. 134, no. 3, pp. 387–401, 2016.

[2] N. W. Arnell and B. Lloyd-Hughes, "The global-scale impacts of climate change on water resources and flooding under new climate and socio-economic scenarios," *Clim Chang*, vol. 122, pp. 127–140, 2014.

[3] A. P. M. Baede, E. Ahlonsou, Y. Ding, and D. S. Schimel, *The climate system: an overview. impacts, adaptation and vulnerability*, Cambridge University Press, New York, 2021, pp. 87–98.

[4] R. S. Tol, "The economic impacts of climate change," *Rev. Environ. Econ. Policy*, vol. 12, no. 1, pp. 4–25, 2018.

[5] A. G. Olabi, "Circular Economy and Renewable Energy," *Energy*, vol. 181, no. 1, pp. 450-454, 2019.

[6] S. Kumar, A. Darshna, and D. Ranjan, "A review of literature on the integration of green energy and circular economy," *Heliyon*, vol. 9, no. 11, 2023, Art. no. e21091.

[7] P. Brzyski, M. Grudzińsk, M. Böhm, and G. Łagód, "Energy Simulations of a Building Insulated with a Hemp-Lime Composite with Different Wall and Node Variants," *Energies*, vol. 15, no. 20, 2022, Art. no. 7678.

[8] M. Kubiś, P. Łapka, Ł. Cieślikiewicz, G. Sahmenko, M. Sinka, and D. Bajare, "Analysis of the Thermal Conductivity of a Bio-Based Composite Made of Hemp Shives and a Magnesium Binder," *Energies*, vol. 5, no. 15, 2022, Art. no. 5490.

[9] J. Henry, "Tropical And Equatorial Climates," in *Encyclopedia of World Climatology*, Springer, Dordrecht, 2005, pp. 742–750.

[10] K. Hamilton, "Dynamics of the tropical middle atmosphere: a tutorial review," *Atmosphere-Ocean*, vol. 36, pp. 319–354, 1998.

[11] A. Allouhi, Y. El Fouih, T. Kousksou, A. Jamil, Y. Zeraouli, and Y. Mourad, "Energy consumption and efficiency in buildings: Current status and future trends," *Journal of Cleaner Production*, 2015, doi: 10.1016/j.jclepro.2015.05.139.

[12] C. W. Thornthwaite, "The climates of North America according to a new classification," *Geographical Review*, vol. 21, pp. 633–655, 1931.

[13] A. Salman, "The Influence of Polyurethane Foam on the Insulation Characteristics of Mortar Pastes," *Journal of Minerals and Materials Characterization and Engineering*, vol. 5, no. 2, 2017, Art. no. 13.

[14] J. Liao, Y. Hou, J. Li, M. Zhang, Y. Dong, and X. Chen, "Lightweight and recyclable hybrid multifunctional foam based cellulose fibers with excellent flame retardant, thermal, and acoustic insulation property," *Composites Science and Technology*, vol. 244, no. 10, 2023, Art. no. 110315.

[15]V. Nuno. Gama, F. Artur, and A. Barros-Timmons, "Polyurethane Foams: Past, Present, and Future," *Materials*, vol. 11, no. 10, 2018, Art. no. 1841.
[16]T.S. Raghu, T.M. Kotresh, R. Indushekar, and K. M. Babu, "Fire Behaviors of Polyurethane Foams," *Indian Journal of Advances in Chemical Science*, vol. 3, pp. 109–112, 2014.
[17]E. Guolo, F. Cappelletti, P. Romagnoni, and F. Raggiotto, "Environmental impacts for polyurethane panels," *Web of Conferences*, 2019, doi: 10.1051/e3sconf/2019111030 201.
[18]M. Król, "Natural vs. Synthetic Zeolites," *Crystals*, vol. 10, no. 7, 2020, Art. no. 622.
[19]F. E. Ayala, Y. Reyes-Vidal, J. Bacame-Valenzuela, J. Pérez-García, A. H. Palomares, "Chapter 25 - Natural and synthetic zeolites for the removal of heavy metals and metalloids generated in the mining industry," in *New Trends in Removal of Heavy Metals from Industrial*, Elsevier, 2021, pp. 63–648.
[20]N. Salahudeen, "A Review on Zeolite: Application, Synthesis and Effect of Synthesis Parameters on Product Properties," *Chemistry Africa*, vol. 5, pp. 1889–1906, 2022.
[21]N. Kordala and M. Wyszkowski, "Zeolite Properties, Methods of Synthesis, and Selected Applications," *Molecules*, vol. 2024, no. 29, 2024, Art. no. 1069.
[22]E. Pérez-Botella. S. Valencia, and F. Rey, "Zeolites in Adsorption Processes: State of the Art and Future Prospects," *Chem. Rev.*, vol. 122, no. 24, pp. 17647–17695, 2022.
[23]F. Changling, E. Jiaqiang, H. Wei, D. Yuanwang, B. Zhang, X. Zhao, and D. Han, "Key technology and application analysis of zeolite adsorption for energy storage and heat-mass transfer process: A review," *Renewable and sustainable energy reviews*, vol. 144, 2021, Art. no. 110954.
[24]T. M. Le, G. T. Nguyen, N. D. Dat, and N. T. Tran, "An innovative approach based on microwave radiation for synthesis of zeolite 4A and porosity enhancement," *Results in Engineering*, vol. 19, 2023, Art. no. 101235.
[25]Z. Y. Liu, G. Cacciola, G. Restuccia, and N. Giordano, "Fast simple and accurate measurement of zeolite thermal conductivity," *Zeolites*, vol. 10, no. 6, pp. 565–570, 1990.
[26]M. Ducamp and C. François-Xavier, "Systematic Study of the Thermal Propertiesof Zeolitic Frameworks," *Journal of Physical Chemistry C*, vol. 125, no. 28, pp.15647–15658, 2021.